Observation of nonadditive mixed state phases with polarized neutrons

Jürgen Klepp[1], Stephan Sponar[1], Stefan Filipp[1], Matthias Lettner[1], Gerald Badurek[1] and Yuji Hasegawa[1,2]

[1] *Vienna University of Technology, Atominstitut, Stadionallee 2, 1020 Vienna, Austria and*

[2] *PRESTO, Japan Science and Technology Agency, 4-1-8 Honcho Kawaguchi, Saitama, Japan*

Abstract

In a neutron polarimetry experiment the mixed state relative phases between spin eigenstates are determined from the maxima and minima of measured intensity oscillations. We consider evolutions leading to purely geometric, purely dynamical and combined phases. It is experimentally demonstrated that the sum of the individually determined geometric and dynamical phase does not yield the total phase as obtained from a single measurement, unless the system is in a pure state.

PACS numbers: 03.65.Vf, 03.75.Be, 42.50.-p

Keywords:

Evolving quantum systems acquire two kinds of phase factors: (*i*) the dynamical phase which depends on the dynamical properties of the system - like energy or time - during a particular evolution, and (*ii*) the geometric phase which only depends on the path the system takes in state space on its way from the initial to the final state. Since its discovery by Pancharatnam [1] and Berry [2] the concept was widely expanded and has undergone several generalizations. Nonadiabatic [3] and noncyclic [4] evolutions as well as the off-diagonal case, where initial and final state are mutually orthogonal [5], have been considered. Ever since, a great variety of experimental demonstrations has been accomplished [6, 7], also in neutron optics [8–11]. Due to its potential robustness against noise [12] the geometric phase is an excellent candidate to be utilized for logic gate operations in quantum information science [13].

Besides other approaches [14] a new concept of mixed state phase based on interferometry was developed by Sjöqvist *et al.* [15]. Here, each eigenvector of the initial density matrix independently acquires a geometric phase. The total mixed state phase is a weighted average of the individual phase factors. It is of great interest for any experimental situation or technical application - where pure state theories may imply strong idealizations - and an important step towards the understanding of nonunitary processes induced by decoherence [16]. Its theoretical predictions have been tested by Du *et al.* [17] and Ericsson *et al.* [18] using NMR and single-photon interferometry, respectively. In this Letter, we report on measurements of nonadiabatic and noncyclic geometric, dynamical and general phases depending on the polarization, i.e. the purity, of the neutron input state arising from various noise levels in state preparation. Furthermore, we show experimentally that the geometric and dynamical mixed state phases Φ_g and Φ_d resulting from separate measurements do not - in one single cumulative measurement - just add up to the total phase as $\Phi_{\rm tot} = \Phi_g + \Phi_d$ [19], as naively expected. This nonadditivity might be of practical importance for applications, e.g. the design of phase gates for quantum computation.

A neutron beam propagating in y-direction interacting with static magnetic fields $\vec{\rm B}(y)$ is described by the Hamiltonian H$= -\hbar^2/2m\vec{\nabla}^2 - \mu\vec{\sigma}\vec{B}(y)$; m and μ are the mass and the magnetic moment of the neutron, respectively. Zeeman splitting within $\vec{\rm B}(y)$ leads to solutions of the Schrödinger equation $\cos(\theta/2)|k_+\rangle|+\rangle + e^{i\alpha}\sin(\theta/2)|k_-\rangle|-\rangle$, where $|k_\pm\rangle$ are the momentum and $|\pm\rangle$ the spin eigenstates within the field $\vec{\rm B}(y)$. θ and α denote the polar and azimuthal angles determining the direction of the spin with respect to $\vec{\rm B}(y)$. $k_\pm \simeq k_0 \mp \Delta k$,

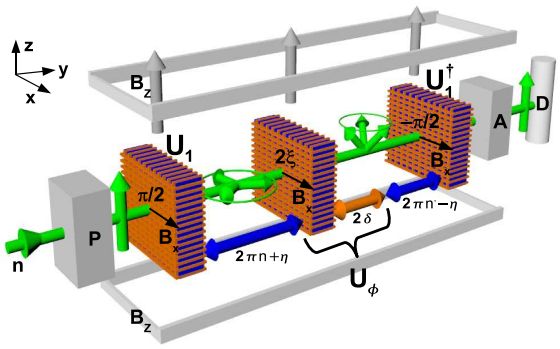

FIG. 1: Sketch of neutron polarimetry setup for phase measurement with overall guide field B_z, polarizer P, three DC-coils to implement unitary operations U_1, $U_1^\dagger$, U_ϕ, analyzer A and detector D. Greek letters denote spin rotation angles. Shifting the second coil induces an additional phase η resulting in intensity oscillations. The desired phase ϕ is determined from their minima and maxima.

where k_0 is the momentum of the free particle and $\Delta k = m\mu|\vec{B}(y)|/\hbar^2 k$ is the field-induced momentum shift due to conservation of total energy. Δk can be detected from the spinor precession it inevitably implies. Omitting the coupling of momentum and spin, we focus on the evolution of the spin state resulting in Larmor precession of the polarization vector $\vec{r} = \langle\varphi|\vec{\sigma}|\varphi\rangle$, where $\vec{\sigma} = (\sigma_x, \sigma_y, \sigma_z)$ is the Pauli vector operator. The unitary, unimodular operator

$$\begin{aligned} \mathrm{U}(\xi', \delta', \zeta') \;&=\; e^{i\delta'} \cos\xi' |+\rangle\langle+| - e^{-i\zeta'} \sin\xi' |+\rangle\langle-| \\ &+\; e^{i\zeta'} \sin\xi' |-\rangle\langle+| + e^{-i\delta'} \cos\xi' |-\rangle\langle-| \end{aligned}$$

describes the evolution of the system within static magnetic fields. The set of SU(2) parameters (ξ', δ', ζ') is related to the so-called Cayley-Klein parameters a, b via $a = e^{i\delta'}\cos\xi'$ and $b = -e^{-i\zeta'}\sin\xi'$ (see e.g. [20]).

Consider the experimental setup shown in Fig. 1. A monochromatic neutron beam passes the polarizer P preparing it in the 'up' state $|\psi_{\mathrm{in}}\rangle = |+\rangle$ with respect to a magnetic guide field in z-direction (B_z). Next the beam approaches a DC coil with its field B_x pointing to the x-direction. B_x is chosen in such a way that it carries out the transformation $U_1 \equiv U(\pi/4, 0, -\pi/2)$, corresponding to a $+\pi/2$ rotation around the $+x$-axis. After U_1 the resulting state of the system is a coherent superposition of two orthogonal spin eigenstates $|\psi_0\rangle = 1/\sqrt{2}(|+\rangle - i|-\rangle)$. A subsequent coil, represented by $U(\xi, 0, -\pi/2)$, is set to cause

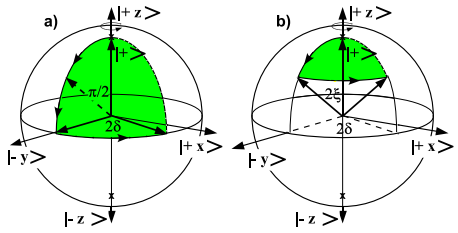

FIG. 2: Evolution of the $|+\rangle$ state induced by U_ϕ, associated to: a) Purely (noncyclic) geometric phase ($2\xi = \pi/2$). b) Combinations of purely dynamical and geometric phase on the Bloch sphere ($0 < 2\xi < \pi/2$).

a spin rotation around the $+x$-axis by an angle 2ξ. This second coil together with the following propagation distance within B_z - corresponding to a rotation angle 2δ around the $+z$-axis - defines an evolution $\mathrm{U}_\phi \equiv \mathrm{U}(\xi, \delta, \zeta)$. Upon undergoing the transformation U_ϕ the two spin eigenstates $|\pm\rangle$ acquire opposite phase $\pm\phi = \pm \arg\langle\psi_{\mathrm{in}}|\mathrm{U}_\phi|\psi_{\mathrm{in}}\rangle = \pm\delta$. A third coil ($\mathrm{U}_1^\dagger$) reverses the action of the first one and would therefore transform a state $|\psi_0\rangle$ back to $|+\rangle$ (clearly, the state of the system entering the third coil equals $|\psi_0\rangle$ only if $\mathrm{U}_\phi = \mathbb{1}$). ϕ can be extracted by applying an extra phase shift $\pm\frac{1}{2}\eta$ to $|\pm\rangle$. It is implemented by elongating the distances from the first to the second and from the second to the third coil to spin rotation angle equivalents of $2\pi n + \eta$ and $2\pi n' + 2\delta - \eta$, respectively, within the field B_z ($n, n' = 0, \pm1, \pm2, ...$). By scanning the position of the second coil the propagation distances between the coils - referred to as $\mathrm{U}_\eta \equiv \mathrm{U}(0, -\eta/2)$ and $\mathrm{U}_\eta^\dagger$ - are varied (note that because of $\xi' = 0$ the parameter ζ' is indetermined and therefore omitted in U_η). After projection on the state $|+\rangle$ by the analyzer A, the phase $\phi = \delta$ and its visibility $\nu = |\langle\psi_{\mathrm{in}}|\mathrm{U}_\phi|\psi_{\mathrm{in}}\rangle| = |\cos\xi|$ can be computed as functions of $\mathrm{I}_{\mathrm{max}}$, $\mathrm{I}_{\mathrm{min}}$ - the maxima and minima of the intensity measured by the detector D [21]. More general, a neutron beam with arbitrary incident degree of polarization $r_0 = |\vec{r}_0|$ along the $+z$-axis ($\vec{r}_0 = (0, 0, r_0)$) is described by the density operator $\rho_{\mathrm{in}}(r_0) = 1/2(\mathbb{1} + r_0\sigma_z)$. Calculating $\rho_{\mathrm{out}} = \mathrm{U}_1^\dagger\mathrm{U}_\eta^\dagger\mathrm{U}_\phi\mathrm{U}_\eta\mathrm{U}_1\rho_{\mathrm{in}}\mathrm{U}_1^\dagger\mathrm{U}_\eta^\dagger\mathrm{U}_\phi^\dagger\mathrm{U}_\eta\mathrm{U}_1$, we find the intensity

$$\begin{aligned} \mathrm{I}^\rho &\propto \mathrm{Tr}(|+\rangle\langle+|\rho_{\mathrm{out}}) \\ &= \frac{1 - r_0}{2} + r_0\left(\cos^2\xi\cos^2\delta + \sin^2\xi\cos^2(\zeta - \eta)\right) \end{aligned} \tag{1}$$

after the analyzer A. Considering the maxima and minima $\mathrm{I}^\rho_{\mathrm{max}}$, $\mathrm{I}^\rho_{\mathrm{min}}$ of η-induced oscillations of I^ρ one obtains the mixed state phase [22]

$$\Phi(r_0) \;=\; \arg \mathrm{Tr}(\mathrm{U}_\phi \rho_{\mathrm{in}}) = \arccos \sqrt{\frac{[\mathrm{I}^\rho_{\mathrm{min}}/\mathrm{I}^\rho_{\mathrm{n}} - 1/2(1-r_0)]/r_0}{r_0[1/2(1+r_0) - \mathrm{I}^\rho_{\mathrm{max}}/\mathrm{I}^\rho_{\mathrm{n}}] + [\mathrm{I}^\rho_{\mathrm{min}}/\mathrm{I}^\rho_{\mathrm{n}} - 1/2(1-r_0)]/r_0}} \quad (2)$$

with a normalization factor $\mathrm{I}^\rho_{\mathrm{n}} = 2\mathrm{I}^\rho_0/(1+r_0)$. I^ρ_0 is the intensity measured at $\mathrm{U}_\phi = \mathbb{1}$.

The noncyclic geometric phase is given by $\phi_g = -\Omega/2$, where Ω is the solid angle enclosed by a geodesic path and its shortest geodesic closure on the Bloch sphere [4]: the phase ϕ_g can be related to the path by the polar and azimuthal angles 2ξ and 2δ, so that the pure state geometric phase becomes

$$\phi_g = \delta[1 - \cos(2\xi)], \quad (3)$$

while its dynamical counterpart is

$$\phi_d = \delta \cos(2\xi). \quad (4)$$

By proper choices of 2ξ and δ, U_ϕ can be set to generate purely geometric, purely dynamical, or arbitrary combinations of both phases as shown in Fig. 2.

The theoretical prediction for the mixed state phase is [15, 22]

$$\Phi(r_0) \;=\; \arctan(r_0 \tan\delta) \quad (5)$$

To access Eq. (5) experimentally r_0 needs to be varied. In addition to the DC current (to achieve the transformation U_1) a random noise signal is applied to the first coil, thereby changing B_x in time. Neutrons which are part of the ensemble $\rho_{\mathrm{in}}(r_0)$ arriving at different times at the coil experience different magnetic field strengths, which is equivalent to applying different unitary operators $\mathrm{U}(\pi/4 + \Delta\xi'(t), 0, -\pi/2) = \mathrm{U}_1(\Delta\xi'(t))$. For the whole ensemble we have to take the time integral

$$\rho = \int \mathrm{U}_1(\Delta\xi'(t))|+\rangle\langle+|\mathrm{U}_1^\dagger(\Delta\xi'(t))dt.$$

Although each separate transformation is unitary, due to the randomness of the signal we end up with a nonunitary evolution that yields a mixed state [23]. Note that in this method the purity of the input state is not affected before U_1, but spin superpositions distributed around $|\psi_0\rangle$ within the y,z-plane are created by U_1. We are left with $\vec{r_0} = (0, -r_0, 0)$ where $r_0 < 1$, as has been confirmed by a 3D spin analysis of the state $|\psi_0\rangle$.

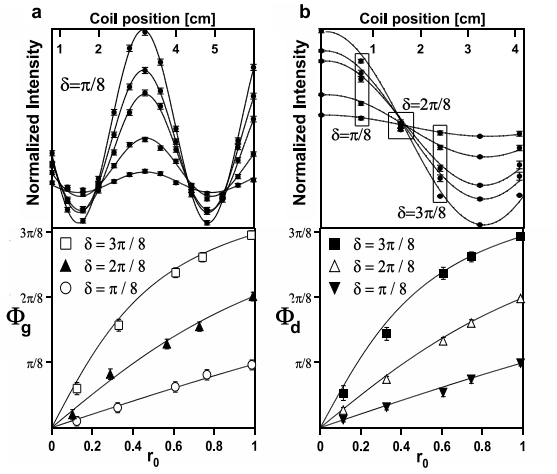

FIG. 3: Above: typical measured intensities for five values of purity r versus coil positions. Below: resulting mixed state phases $\Phi_g(r_0)$ and $\Phi_d(r_0)$ versus purity r_0. a) Purely geometric case: $2\xi = \pi/2$. b) Purely dynamical case: $2\xi = 0$. Only one intensity value is needed to yield Φ_d (see text). Intensity values marked by rectangles correspond to $\delta = \phi_d = \pi/8, 2\pi/8, 3\pi/8$.

The experiment was carried out at the research reactor facility of the Vienna University of Technology. A neutron beam of mean wavelength $\lambda \approx 1.98\,\text{Å}$ and spectral width $\Delta\lambda/\lambda \approx 0.015$, incident from a pyrolytic graphite monochromator, was polarized up to $r_0 \approx 99\,\%$ by reflection from a bent Co-Ti supermirror array. The analyzing supermirror was slightly de-adjusted to higher reflection angles to suppress second order harmonics in the incident beam. The final maximum intensity was about 150 counts/s at a beam cross-section of 1 cm. A ^{3}He gas detector with high efficiency for neutrons of this energy range was used in the experiment. Spin rotations around the $+x$-axis were implemented by magnetic fields B_x from DC coils made of anodized aluminium wire (0.6 mm in diameter) wound on frames with rectangular profile ($7\times7\times2$ cm^3). Coil windings in z-direction provided for compensation of the guide field B_z at coil positions (see Fig. 1) providing for B_x to be parallel to the x-direction. B_z was realized by two rectangular coils of 150 cm length in Helmholtz geometry. Coil currents of 2 A maximum and guide field strengths of 1 mT were sufficient to achieve required rotations and prevent unwanted depolarization. The random noise signal from a standard signal generator consisted of random DC offsets varying at a rate of 20 kHz. In order to find the coil current values corresponding to required spin rotation angles, all currents were scanned separately: starting from zero current, an intensity minimum behind

the analyzer after stepwise increase indicates that a π rotation has been achieved. The distance within B_z between two particular coils was related to rotation angles by measuring the intensity as a function of the position of one coil (mounted on a translation stage) with both coils set to a rotation of $\pi/2$ around the x-axis. The distance between two minima (6-7 cm in our case) corresponds to a 2π rotation within the x, y plane.

For purely geometric phases the parameter sets ($\xi = \pi/4, \delta, \zeta = \delta - \pi/2$) with $\delta = \phi_g = \pi/8, 2\pi/8, 3\pi/8$ were chosen. For each set the intensity oscillations I^ρ (see Fig. 3a, upper graph; data shown for $\delta = \phi_g = \pi/8$) were measured, scanning the position of the second coil for five values of r_0. For the purely dynamical phase - where $2\xi = 0$ and Eq. (1) reduces to $I^\rho = (1-r_0)/2 + r_0 \cos^2 \delta$ - only one intensity value is needed. With the second coil turned off, the distance between the first and the third coil was chosen such that $\delta = \phi_d = \pi/8, 2\pi/8, 3\pi/8$ for five values of r_0 (Fig. 3b, upper graph). By Eq. (2) the geometric and dynamical mixed state phases $\Phi_d(r_0)$ and $\Phi_g(r_0)$ (Fig. 3, lower graphs) were calculated from the minima and maxima of least square fits to I^ρ (in Fig. 3, upper graphs). The solid lines are theoretical curves according to Eqs. (5), using the measured value for Φ at $r_0 \approx 1$ as phase reference. The experimental data reproduce well the r_0-dependence predicted by Eqs. (5).

In particular, we have investigated a special property of the mixed state phase in our experiments: its nonadditivity. Since the Sjöqvist phase is defined as a weighted average of phase factors rather then one of phases (see [19, 24] for a more elaborate discussion) it is only for the pure state case that phases of separate measurements can be added up to a total phase. Suppose we carry out a measurement on a system in a pure state undergoing some unitary transformation U_g inducing a pure state phase ϕ_g and another measurement for the same system undergoing U_d that induces ϕ_d. We can choose a combination of angles 2ξ and 2δ leading to a transformation $U_{\rm tot}$ so that we measure the total pure state phase $\phi_g + \phi_d$. However, the result of the same experiment for the system in a mixed state ($r_0 < 1$) is $\Phi_{\rm tot}(r_0) = \arctan\left[r_0 \tan(\phi_g + \phi_d)\right]$. The total phase is *not* given by $\Phi_g(r_0) + \Phi_d(r_0)$ (with $\Phi_g(r_0) = \arctan\left(r_0 \tan \phi_g\right)$ and $\Phi_d(r_0) = \arctan\left(r_0 \tan \phi_d\right)$, the results of two separate measurements), as one could intuitively expect. In our experiment we have chosen two examples of $U_{\rm tot}$, i.e. two sets of values for B_x in the second coil ($2\xi^{(1)} = 60^\circ,\ 2\xi^{(2)} = 48.18...^\circ$) and the distance within B_z ($2\delta^{(1)} = 90^\circ,\ 2\delta^{(2)} = 135^\circ$). According to Eqs. (3) and (4) the total pure state phases $\phi_g^{(1)} + \phi_d^{(1)}$ and $\phi_g^{(2)} + \phi_d^{(2)}$ with $\phi_g^{(1)} = \phi_g^{(2)} = \pi/8$ and $\phi_d^{(1,2)} = 2\pi/8, \pi/8$ are obtained from intensity oscillations. In Fig. 4 the resulting mixed state phase $\Phi_{\rm tot}(r_0)$

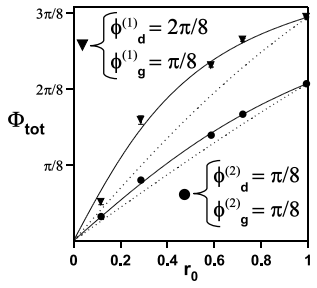

FIG. 4: Measured total mixed state phase $\Phi_{\rm tot}(r_0)$ versus purity r_0 for two examples of $\mathrm{U}_{\rm tot}^{(1,2)}$ associated to the total pure state phases $\phi_g^{(1,2)} + \phi_d^{(1,2)}$ (see text). The data clearly demonstrates the nonadditivity of the Sjöqvist mixed state phase.

is plotted versus the purity r_0. The solid lines are theoretical curves according to Eq. (5). The dotted lines correspond to $\Phi_g(r_0) + \Phi_d(r_0)$ for either example. Of course, the argument given above is valid not only for a sum of dynamical and geometric phases - which is what we have shown here - but for general mixed state phases. Note also that this nonadditivity of the mixed state phase is not due to the nonlinearity of the geometric phase, occurring - for instance - when the system evolves close to the state orthogonal to its reference state [25].

Recently there has been a report on NMR experiments [26] investigating Uhlmann's mixed state geometric phase. It is a property of a composite system undergoing a certain non-local evolution of a system and its ancilla [27]. Diverse phase definitions are possible, depending on this evolution. The phase investigated in the present paper is a special case in which the ancilla does not necessarily evolve. It is independent of the evolution of the entangled ancilla. The question whether other phases offer advantages in terms of robustness remains an exciting issue of discussion.

To summarize, we have measured spin-1/2 mixed state phases with polarized neutrons. The dependence of the phase on the purity r_0 was observed for purely dynamical and purely geometric phases, as well as combinations of both. Our results also show that mixed state phases are not additive, i.e. the sum of phases measured in separate experiments is not equal to the result of one single measurement, as one could expect from straightforward expansion from familiar pure state behavior. This interesting property of the mixed state phase might be of high relevance for possible applications of geometric phases.

This work was financed by the Japan Science and Technology Agency (JST) and the

Austrian Science Fund (FWF, Project. Nr. P 17803-N02).

[1] Pancharatnam, Proc. Indian Acad. Sci. A **44** (1956).

[2] M.V. Berry, Proc. R. Soc. Lond. A **392**, 45 (1984).

[3] Y. Aharonov and J.S. Anandan, Phys. Rev. Lett. **58**, 1593 (1987).

[4] J. Samuel and R. Bhandari, Phys. Rev. Lett. **60**, 2339 (1988).

[5] N. Manini and F. Pistolesi, Phys. Rev. Lett. **85**, 3076 (2000).

[6] A. Tomita and R.Y. Chiao, Phys. Rev. Lett. **57**, 937 (1986).

[7] D. Suter, K.T. Mueller and A. Pines, Phys. Rev. Lett. **60**, 1218 (1988).

[8] T. Bitter and D. Dubbers, Phys. Rev. Lett. **59**, 251 (1987).

[9] B.E. Allman, H. Kaiser, S.A. Werner, A.G. Wagh, V.C. Rakhecha and J. Summhammer, Phys. Rev. A **56**, 4420 (1997).

[10] Y. Hasegawa, R. Loidl, M. Baron, G. Badurek and H. Rauch, Phys. Rev. Lett. **87**, 070401 (2001).

[11] S. Filipp, Y. Hasegawa, R. Loidl and H. Rauch, Phys. Rev. A **72**, 021602(R) (2005).

[12] P.J. Leek, J.M. Fink, A. Blais, R. Bianchetti, M. Göppl, J.M. Gambetta, D.I. Schuster, L. Frunzio, R.J. Schoelkopf and A. Wallraff, Science **318**, 1889 (2008).

[13] M.A. Nielsen and I.L. Chuang, *Quantum Computation and Quantum Information*, Cambridge University Press, Cambridge, England, 2000.

[14] A. Uhlmann, Lett. Math. Phys. **21**, 229 (1991).

[15] E. Sjöqvist, A.K. Pati, A. Ekert, J.S. Anandan, M. Ericsson, D.K.L. Oi and V. Vedral, Phys. Rev. Lett. **85**, 2845 (2000).

[16] E. Joos, H.D. Zeh, C. Kiefer, D. Giulini, J. Kupsch and I.-O. Stamatescu, *Decoherence and the Appearance of a Classical World in Quantum Theory* (Springer, Heidelberg, 2003)

[17] J. Du, P. Zou, M. Shi, L.C. Kwek, J.-W. Pan, C.H. Oh, A. Ekert, D.K.L. Oi and M. Ericsson, Phys. Rev. Lett. **91**, 100403 (2003).

[18] M. Ericsson, D. Achilles, J.T. Barreiro, D. Branning, N.A. Peters and P.G. Kwiat, Phys. Rev. Lett. **94**, 050401 (2005).

[19] K. Singh, D. M. Tong, K. Basu, J. L. Chen and J. F. Du, Phys. Rev. A **67**, 032106 (2003).

[20] J.J. Sakurai, *Modern Quantum Mechanics* (Addison-Wesley, New York, 1994)

[21] A.G. Wagh and V.C.Rakhecha, Phys. Lett. A **197**, 112 (1995).

[22] P. Larsson and E. Sjöqvist, Phys. Lett. A **315**, 12 (2003); J. Klepp, S. Sponar, Y. Hasegawa, E. Jericha and G. Badurek, Phys. Lett. A **342**, 48 (2005); S. Sponar, J. Klepp, Y. Hasegawa, E. Jericha and G. Badurek, Acta Phys. Hung. A **26**, 165 (2006).

[23] R.A. Bertlmann, K. Durstberger and Y. Hasegawa, Phys. Rev. A **73**, 022111 (2006)

[24] Li-Bin Fu and Jing-Ling Chen, J. Phys. A: Math. Gen. **37**, 3699 (2004). E. Sjöqvist, J. Phys. A: Math. Gen. **37**, 7393 (2004). Li-Bin Fu and Jing-Ling Chen, J. Phys. A: Math. Gen. **37**, 7395 (2004).

[25] R. Bhandari, Phys. Rep. **281**, 1 (1997).

[26] J. Du, M. Shi, J. Zhu, V. Vedral, X. Peng and D. Suter, arXiv:0710.5804v1 [quant-ph].

[27] M. Ericsson, A. K. Pati, E. Sjöqvist, J. Brännlund and D. K. L. Oi, Phys. Rev. Lett. **91**, 090405 (2003).